
Article:
Zhong, Hai, Tarrach, Guido, Wu, Peiwen et al. (3 more authors) (2008) High resolution magnetic force microscopy of patterned L1(0)-FePt dot arrays by nanosphere lithography. Nanotechnology. 095703. ISSN 0957-4484

https://doi.org/10.1088/0957-4484/19/9/095703

Nanotechnology **19** (2008) 095703 (5pp) doi:10.1088/0957-4484/19/9/095703

High resolution magnetic force microscopy of patterned $L1_0$-FePt dot arrays by nanosphere lithography

Hai Zhong[1], Guido Tarrach[2], Peiwen Wu[1], Andreas Drechsler[2], Dan Wei[1] and Jun Yuan[1,3,4]

[1] Laboratory of Advanced Materials, Department of Materials Science and Engineering, Tsinghua University, Beijing 100084, People's Republic of China
[2] SwissProbe Ltd, Klingelbergstrasse 82, CH-4056 Basel, Switzerland
[3] Department of Physics, University of York, Heslington, York YO10 5DD, UK

E-mail: yuanjun@mail.tsinghua.edu.cn

Received 22 November 2007, in final form 20 December 2007
Published 12 February 2008
Online at stacks.iop.org/Nano/19/095703

Abstract

High resolution magnetic force microscopy (MFM) has been carried out on $L1_0$-FePt dot arrays patterned by plasma modified nanosphere lithography. An *ex situ* tip magnetization reversal experiment is carried out to determine the magnetic domains and verify the imaging stability of MFM and the mutual perturbations between the magnetic tip and the sample. We have identified that the critical size for the single domain region is about 90 nm across. Comparison with MFM image simulation also suggests that the magnetizations of the triangular dots in both single and double domain states are parallel to one edge of the dots, indicating the large uniaxial magnetocrystalline anisotropy of the $L1_0$-FePt phase and the need for decreasing the magnetostatic energy.

(Some figures in this article are in colour only in the electronic version)

1. Introduction

Patterned magnetic nanostructures, such as two-dimensional dot arrays, have attracted a great deal of interest due to their potential applications in many technologically important fields, such as magnetic information storage [1] or non-volatile magnetic random access memory (MRAM) [2]. As the physical size of the nanoelements in the patterned array decreases, loss of data due to the thermal instability (also known as 'superparamagnetic effect') would become a very crucial issue [3]. To conquer this effect, large uniaxial magnetic anisotropy (K_u) materials, such as the $L1_0$ phase of FePt with a theoretical value of $K_u \sim 7.0 \times 10^7$ erg cm^{-3} [4], would become a promising candidate. Large scale production of arrays of $L1_0$-FePt nanoelements is still a challenge. Currently, patterned $L1_0$-FePt nanoelements (or nanoparticles) can be produced either by self-assembly of chemically prepared FePt monodisperse nanoparticles [5], or by patterning FePt films using electron beam lithography (EBL) [6]. The self-assembly method requires post-deposition annealing to transform the as-deposited chemically disordered face-centered cubic (fcc) structure into the chemically ordered face-centered tetragonal (fct) phase ($L1_0$-phase). Random nucleation in the initial stages of the $L1_0$-phase growth could result in broad distributions of particle sizes, which may be further aggravated by agglomeration during annealing [5]. The EBL method is an expensive and time-consuming direct-writing technique, which is not suitable for mass production [7]. Recently, we have shown that a lithographic method using a plasma modified nanosphere self-assembly template can be used to produce a regular array of such $L1_0$-FePt nanoelements in a large scale [8]. In this method, the interstitial voids in the nanosphere template are modified by plasma etching and used to deposit FePt multilayers at room temperature. Post-annealing then promotes the desired order–disorder transition while preserving the dot structure [9]. A detailed structure analysis of the FePt dots has been previously reported in reference [9], in which a low resolution MFM result is also shown. The low resolution MFM was carried out

[4] Author to whom any correspondence should be addressed.

in a conventional tapping/lift mode, where the topographical information was obtained in the first tapping mode scan and the phase variation was recorded as magnetic contrast in the second scan with a preset lift height following the previous topographical trace. The resolution of the MFM by the tapping/lift mode is inherently limited by the tip used, which could be easily damaged at the nanometer scale during the tapping mode scan. The phase variation is also difficult to interpret because it is a combination of damping and force gradient in a non-linear way [10]. By operating a dynamical MFM in the constant height mode, we can achieve high resolution using an ultrasharp tip that does not need to touch the sample surface. The frequency shift measured is commonly assumed to be proportional to the force derivative [11], and can be more easily compared to theoretical simulation. We have shown that the $L1_0$-FePt dots contain clearly resolved magnetic fine structures. The good agreements between the experimental and simulated MFM images indicate that the dots are indeed in-plane magnetized with the magnetic moments lying along one edge of the triangle shape, possibly due to the need for decreasing the magnetostatic energy. Our MFM results also indicate that the in-plane critical single domain size for such $L1_0$-FePt dots is about 90 nm. Our results provide useful information for the further development of FePt based patterned media.

2. Experimental details

Our method to fabricate patterned magnetic media is to use ion-beam etched bilayer nanosphere templates as masks for FePt multilayer deposition at room temperature, which is followed by the removal of nanosphere templates and a post-annealing process [9]. The template utilizes the self-assembly of monodisperse polystyrene nanospheres as an inverse pattern whose deposition channels are defined by interstitial voids between nanospheres. We use an ion beam etching process for the controlled opening of the deposition channels, and hence to prepare arrays of variable size (from ∼20 to 100 nm) nanodots by evaporation through such templates [8].

A multilayer, $Fe_{3\ nm}/(Fe_{1\ nm}/Pt_{1\ nm})_9/Pt_{3\ nm}$, with a total nominal thickness of 24 nm, was deposited onto an oxidized surface of a silicon wafer through a bilayer nanosphere lithographic template [8] by electron beam evaporation at room temperature. The nanosphere template was removed by rinsing in acetone. The patterned FePt dot array was then annealed in H_2 atmosphere at 550 °C for 20 min to promote the disorder-to-order transition [12]. The detailed structural characterization can be found in [13]. Here a summary is given. The ordered $L1_0$ crystalline structure of the FePt dot array was confirmed by x-ray diffraction after annealing. The energy dispersive spectrometer (EDS) in an SEM (scanning electron microscope) indicated that the composition of FePt dots was $Fe_{45}Pt_{55}$. The magnetization loop of the FePt dots after annealing was measured by a superconducting quantum interference device (SQUID) at room temperature, and indicated mostly in-plane magnetization with a coercivity of ∼2.5 kOe.

In this study, the morphology and magnetic properties of $L1_0$-FePt dot arrays were examined in the same scanning probe microscope (Swissprobe, hr-MFM) at room temperature. The former experiment was operated using a contact mode AFM (atomic force microscope) in ambient conditions with a high aspect ratio (HAR) silicon tip (the apex curvature radius is less than 10 nm), while the latter was performed in the constant height mode MFM in high vacuum conditions (base pressure less than 1.0×10^{-5} mbar) with an HAR low-moment magnetic tip (coated by Co alloy; the total apex curvature radius is also ∼10 nm). In this MFM mode, the tip was scanned in a plane parallel to the nominal sample surface without z-feedback, and the overall tip–sample force was measured. The electrostatic contribution to the tip–sample force was compensated by applying a bias voltage between the tip and the sample [14]. The MFM images containing both the magnetic and topographic contributions were then acquired twice at the same tip–sample distance by an *ex situ* tip magnetization reversal approach [15]. Consequently, the two contributions can be completely separated by summation and subtraction of the two images with inverted tip magnetizations. The sample was magnetized from the bottom of a permanent magnet (∼0.4 T field) in the normal direction before acquisition of the MFM images.

3. Results and discussion

Figure 1(a) shows the AFM morphology of the individual dots within the array. They are triangular prism like, corresponding to the typical shape of the etched holes of the bilayer nanosphere template [8]. The non-equilateral triangle of the prism base may be due to the misorientation of the template covered substrate during the etching or evaporation processes [16]. In addition, we could also see a Y-shape dot cluster, which is caused by a defect in the bilayer nanosphere template. The interdot distance of 200 nm is consistent with the size of the nanospheres used. The convolution between the tip and sample would make the edges of the dots smoother. As a result, the contact mode AFM measurement of the radial dimension of ∼70 nm is probably an overestimate of the actual dot size, but we expect that the height measurement should still be very accurate. The statistical distribution of the measured dot heights (figure 1(b)) can be fitted by a Gaussian function with a mean value of about 31 nm, with a full width at half maximum (FWHM) of 3.6 nm.

Figures 1(c) and (d) show the high resolution MFM images of the $L1_0$-FePt dot array in remanent magnetic states with opposite tip magnetizations (upwards and downwards). In both cases, the scan heights are controlled to be nearly the same and just 10 nm above the highest point in the sample. We can separate the topographic and magnetic contributions by summing and subtracting of figures 1(c) and (d). However, the non-magnetic (mostly van der Waals) contribution is estimated to be only 10% of the total measured contrast and hence could be approximately neglected. The weakness of the topographic contribution to the image contrast is understandable as only the highest positions of the rough surface make significant contributions. Given the dominance of the magnetic force contribution to the two MFM images, the nearly exact reversal of the magnetic contrasts as shown in figures 1(c) and (d)

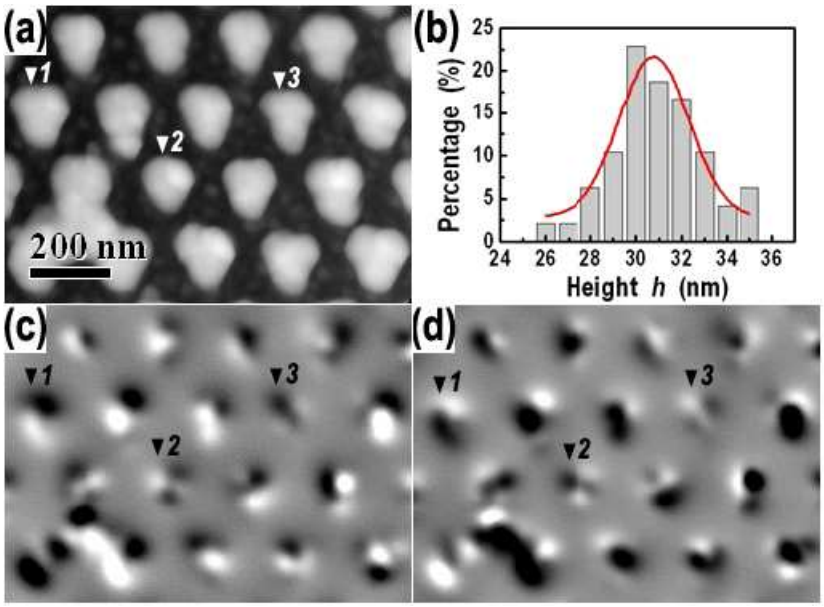

Figure 1. Contact mode AFM and non-contact MFM images of the annealed $L1_0$-FePt dots are shown in (a) and (c)–(d), respectively. The tip magnetization direction is upwards in (c) and downwards in (d). The dot height distribution measured by contact mode AFM is plotted in (b), and can be fitted to a Gaussian function with a mean value of 31 nm and an FWHM of 3.6 nm.

confirms the stability of the magnetizations of both the low-moment magnetic tip and the sample measured in our experiment. Judging by the FWHM peak-to-peak intensity, the MFM image has a lateral resolution of 25 nm. The resolution is much higher than our previous tapping/lift mode MFM result with a resolution of about 80 nm [9]. This helps to reveal the intradot magnetic fine structure clearly.

In the two MFM images (figures 1(c) and (d)), it can be seen that about one half of these $L1_0$-FePt dots show a characteristic black–white dipole contrast (such as dot 1 shown in figure 1(c)) and the rest show a more complex magnetic contrast (i.e., dot 2 or dot 3 shown in figure 1(c)). In particular, the Y-shape cluster has a very complicated multi-domain structure (shown in figures 1(c) and (d)), which is used as a special mark for locating our region of interest in the *ex situ* tip magnetization reversal experiment.

One way to understand the micromagnetic state of the $L1_0$-FePt dots is to compare the MFM images with those of the simulation. The geometrical shape of the nanodots is modeled as a non-equilateral triangular (i.e., isosceles triangle) prism whose base is characterized by two parameters R_1 and R_2; the prism height is characterized by h, as labeled in figure 2(a). As the lateral dimension measured by the contact mode AFM would be larger than the real case because of the convolution with the tip, the statistical distributions of the lateral dimensions R_1 and R_2 are obtained by examining the corresponding SEM results instead [13]. In figure 2(b), the distributions of R_1 and R_2 are fitted by Gaussian distributions; the mean values for R_1 and R_2 are 93 nm (FWHM = 9.6 nm) and 73 nm (FWHM = 11.8 nm), respectively. Comparing the values measured with the SEM with the corresponding AFM measurements (average $R_1 \sim 150$ nm and average $R_2 \sim 130$ nm) one can deduce that the AFM tip contributes about 50 nm in convoluted width.

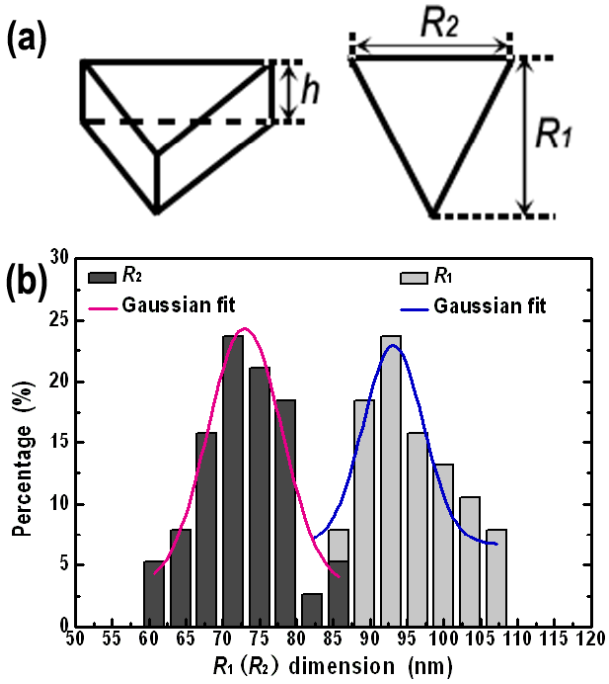

Figure 2. (a) Geometrical model of the $L1_0$-FePt dot as a triangular prism with a height h and a lateral dimension characterized by two parameters R_1 and R_2. (b) Distributions of the lateral dimensions R_1 (gray columns) and R_2 (black columns) from SEM measurements. The solid lines are Gaussian fits to the distributions and the results indicate that R_1 and R_2 have a mean value of 93 nm and 73 nm with an FWHM of 9.6 nm and 11.8 nm, respectively.

In the simulation we have simply assumed the tip to be an effective magnetic point dipole [17] in the z-direction, because an ultrasharp and also HAR MFM tip is used in

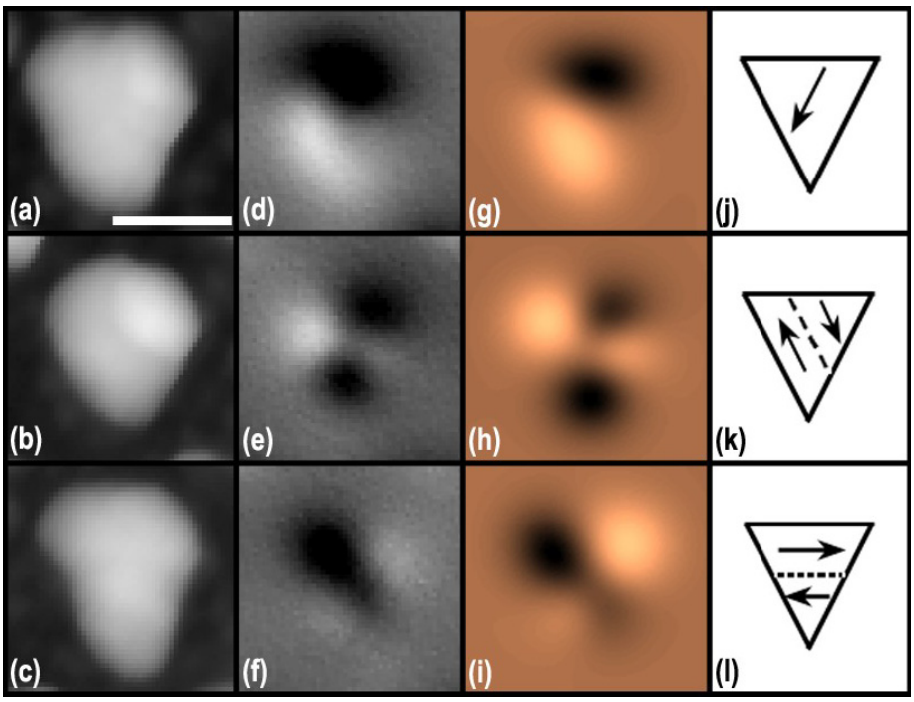

Figure 3. (a)–(c) Contact mode AFM images of the dots highlighted in figure 1(a). The corresponding MFM images taken from figure 1(c) are replotted as (d)–(f) to be compared with the simulated MFM images shown in (g)–(i), based on the single and two different double domain structures shown in (j)–(l), respectively. The scale bar in (a) indicates a length of 100 nm and is also the same for (b)–(i).

our experiment. The measured MFM signal Δf is then approximately sensitive to the second-order derivative of the z-component of the stray field, $\partial^2 H_z/\partial z^2$ [18]. We also assume that the magnetizations are uniform within all the domains. The magnetostatic stray field $\mathbf{H}(\mathbf{r})$ is determined by $\mathbf{H}(\mathbf{r}) = -\tilde{\mathbf{N}}(\mathbf{r}) \cdot \mathbf{M}$, where $\tilde{\mathbf{N}}(\mathbf{r})$ is a magnetostatic interaction tensor (also called the 'demagnetizing matrix') and $\mathbf{M}$ is the uniform magnetization within a domain [19]. By numerically calculating the demagnetizing matrix of the triangular prism shape (as modeled in figure 2(a)) and working out the second-order derivative $\partial^2 H_z/\partial z^2$ above it, we could then obtain the simulated MFM images.

The experimental MFM images of three $L1_0$-FePt dots with three typical domain structures highlighted by arrows and numbered in figure 1(c) are replotted in figures 3(d)–(f). We could observe that the corresponding contact mode AFM images (figures 3(a)–(c)) have a larger tip convolution effect than the MFM images measured in the constant height mode. The corresponding simulated results are shown in figures 3(g)–(i), calculated based on the domain configurations shown in figures 3(j)–(l) by assuming abrupt 180° domain walls (which is reasonable because the domain wall width of $L1_0$-FePt is only ∼3.9 nm [20]). The geometrical parameters of the triangular prism are $R_1 = 93$ nm, $R_2 = 73$ nm and $h = 31$ nm for all the cases shown in figures 3(j)–(l). An adjustable parameter is the distance between the effective magnetic point dipole and the top of the dots. A value of 60 nm is found to show good agreement with the experimental data, which is reasonable compared to the experimental scan height of about 10 nm above the highest position of the sample, indicating that the effective magnetic point dipole is indeed located somewhere within the magnetically active tip volume [17]. The positions of the domain wall in figures 3(k) and (l) are also adjusted in the simulation to obtain the best agreement with the experimental results.

The remarkable agreement of the simulated images with the experimental MFM results implies that the dot in figure 3(d) is in a single domain (SD) state and the dots in figures 3(e) and (f) have double domain (DD) structures with anti-parallel magnetic moments within the two adjacent domains consisting with the domain structures of uniaxial magnetocrystalline anisotropic materials [21], such as $L1_0$-FePt. However, this is in great contrast to the flux closure domain structure observed on triangular dots made of permalloy [22], which has a very weak magnetocrystalline anisotropy. Regardless of SD or DD cases, we could observe that the in-plane magnetizations within the dots tend to be parallel to one of the edges of the triangular shape to reduce free magnetic charges for lowering the magnetostatic energy [23]. It is worth mentioning here that, although the sample was magnetized in a normal magnetic field before the acquisition of the MFM images, the MFM results indicate in-plane magnetization within the $L1_0$-FePt dots. This is contrary to the observation of perpendicular magnetization in continuous FePt thin film processed under a similar condition [12]. The exact reason requires further investigation.

The observation of a mixture of SD and DD dots in figures 1(c) and (d) suggests that the dot size of ∼90 nm is close to the critical value for the single domain state. The transition from a double domain to a single domain state is not expected to be clear cut, given the fluctuation of the shape and size of the dots. It is interesting to note that the

critical single domain size of our in-plane magnetized $L1_0$-FePt dots is about half the previously reported values (about 180–340 nm) [24, 25] for out-of-plane magnetized dots. The difference is worthy of further investigation.

4. Conclusions

Using high resolution MFM, we have successfully characterized the magnetic fine structures of an $L1_0$-FePt dot array prepared by post-annealing of the FePt multilayers patterned by nanosphere lithography. The $L1_0$-FePt dots in the array are found in a mixture of single domain and double domain states, which indicates that the critical single domain size is about 90 nm. The comparison between the experimental and simulated MFM images indicates that typical domain features have mostly an in-plane magnetization with the magnetizations arranged mainly along one edge of the triangle shape, possibly due to the need for decreasing the magnetostatic energy.

Acknowledgments

The work is supported by the Chinese Ministry of Science and Technology (Basic Research Grant 2002CB613501), the National High Technology Research and Development Program of China (Grant 2002AA302103) and the Changjiang Scholar program of the Chinese Ministry of Education.

References

[1] Terris B D and Thomson T 2005 *J. Phys. D: Appl. Phys.* **38** R199
[2] Guo Y M *et al* 2005 *J. Appl. Phys.* **97** 10P506
[3] Weller D and Moser A 1999 *IEEE Trans. Magn.* **35** 4423
[4] Ovanov O A, Solina L V, Demshina V A and Magat L M 1973 *Phys. Met. Metallogr.* **35** 81
[5] Sun S H, Murray C B, Weller D, Folks L and Moser A 2000 *Science* **287** 1989
[6] Seki T, Shima T, Yakushiji K, Takanashi K, Li G Q and Ishio S 2005 *IEEE Trans. Magn.* **41** 3604
[7] Belotti M, Torres J, Roy E, Pepin A, Gerace D, Andreani L C, Galli M and Chen Y 2006 *Microelectron. Eng.* **83** 1773
[8] Wu P W, Peng L Q, Tuo X L, Wang X G and Yuan J 2005 *Nanotechnology* **16** 1693
[9] Wu P W, Fang Y K, Tuo X L, Wang X G, Han B S and Yuan J 2007 *Chin. Sci. Bull.* **52** 1125
[10] Garcia R, Magerle R and Perez R 2007 *Nat. Mater.* **6** 405
[11] Hug H J *et al* 1998 *J. Appl. Phys.* **83** 5609
[12] Wu P, Hu X, Qian J and Yuan J 2006 *Rare Met.* **25** 260
[13] Wu P 2005 *Master Thesis* Tsinghua University, Beijing
[14] Guggisberg M, Bammerlin M, Loppacher C, Pfeiffer O, Abdurixit A, Barwich V, Bennewitz R, Baratoff A, Meyer E and Guntherodt H J 2000 *Phys. Rev.* B **61** 11151
[15] Zhong H, Peng W, Tarrach G, Drechsler A, Wei D and Yuan J 2007 *J. Phys. D: Appl. Phys.* submitted
[16] Zhang G, Wang D Y and Mohwald H 2007 *Nano Lett.* **7** 127
[17] Hartmann U 1989 *Phys. Lett.* A **137** 475
[18] Wiesendanger R and Guntherodt H J 1992 *Scanning Tunneling Microscopy II* (Heidelberg: Springer)
[19] Bertram N N 1994 *Theory of Magnetic Recording* (Cambridge: Cambridge University Press)
[20] Weller D, Moser A, Folks L, Best M E, Lee W, Toney M F, Schwickert M, Thiele J U and Doerner M F 2000 *IEEE Trans. Magn.* **36** 10
[21] Chikazumi S 1964 *Physics of Magnetism* (Tokyo: Wiley)
[22] Kundrotaite A, Rahman M, Aitchison P R and Chapman J N 2001 *Microelectron. Eng.* **57/58** 975
[23] Chou S Y 1997 *Proc. IEEE* **85** 652
[24] Li G Q, Takahoshi H, Ito H, Saito H, Ishio S, Shima T and Takanashi K 2003 *J. Appl. Phys.* **94** 5672
[25] Weller D and Doerner M F 2000 *Annu. Rev. Mater. Sci.* **30** 611